Magnetoresistance oscillations in multilayer systems: Triple quantum wells

S. Wiedmann,[1,2] N. C. Mamani,[3] G. M. Gusev,[3] O. E. Raichev,[4] A. K. Bakarov,[5] and J. C. Portal[1,2,6]
[1]*LNCMI–CNRS, UPR 3228, BP 166, 38042 Grenoble Cedex 9, France*
[2]*INSA Toulouse, 31077 Toulouse Cedex 4, France*
[3]*Instituto de Física, Universidade de São Paulo, CP 66318, CEP 05315-970 São Paulo, SP, Brazil*
[4]*Institute of Semiconductor Physics, NAS of Ukraine, Prospekt Nauki 45, 03028 Kiev, Ukraine*
[5]*Institute of Semiconductor Physics, Novosibirsk 630090, Russia*
[6]*Institut Universitaire de France, 75005 Paris, France*
(Received 30 September 2009; published 4 December 2009)

Magnetoresistance of two-dimensional electron systems with several occupied subbands oscillates owing to periodic modulation of the probability of intersubband transitions by the quantizing magnetic field. In addition to previous investigations of these magnetointersubband (MIS) oscillations in two-subband systems, we report on both experimental and theoretical studies of such a phenomenon in three-subband systems realized in triple quantum wells. We show that the presence of more than two subbands leads to a qualitatively different MIS oscillation picture, described as a superposition of several oscillating contributions. Under a continuous microwave irradiation, the magnetoresistance of triple-well systems exhibits an interference of MIS oscillations and microwave-induced resistance oscillations. The theory explaining these phenomena is presented in the general form, valid for an arbitrary number of subbands. A comparison of theory and experiment allows us to extract temperature dependence of quantum lifetime of electrons and to confirm the applicability of the inelastic mechanism of microwave photoresistance for the description of magnetotransport in multilayer systems.

DOI: 10.1103/PhysRevB.80.245306 PACS number(s): 73.40.−c, 73.43.−f, 73.21.−b

I. INTRODUCTION

Studies of magnetoresistance, in particular, the investigation of Shubnikov-de Haas (SdH) oscillations in semiconductors and metals is an important tool for gathering information about band structure, quantum lifetimes of electrons and interaction mechanisms.[1] In two-dimensional (2D) electron systems, the SdH oscillations occur because of a periodic modulation of electron scattering as the Landau levels consecutively pass through the Fermi level. With increasing temperature, when the thermal broadening of the Fermi distribution exceeds the cyclotron energy $\hbar\omega_c$, the SdH oscillations are strongly damped. In quantum wells with at least two occupied 2D subbands, the magnetoresistance exhibits another kind of oscillating behavior, the so-called magnetointersubband (MIS) oscillations.[2] These oscillations occur because of a periodic modulation of the probability of transitions between the Landau levels belonging to different subbands. The MIS oscillation peaks correspond to the subband alignment condition $\Delta = n\hbar\omega_c$, where Δ is the subband separation, because the isoenergetic (elastic) scattering of electrons between the Landau levels is maximal under this condition. Since the origin of the MIS oscillations is not related to the position of Landau levels with respect to the Fermi energy, these oscillations survive at high temperatures when the SdH oscillations are completely damped. Early experimental studies of MIS oscillations have been carried out in single quantum wells with two populated 2D subbands.[3–5] Recently, MIS oscillations with large amplitudes have been observed and investigated in two-subband systems based on double quantum wells (DQWs).[6,7] The DQWs appear to be the most convenient systems for experimental studies of this phenomenon, because the two-subband occupation is attainable at relatively small electron densities, the electron mobility is high, and a strong tunnel coupling between the wells enables a high probability of intersubband scattering. The studies of MIS oscillations in DQWs provide information about temperature dependence of the quantum lifetime of electrons in the region where SdH oscillations are absent.[6]

The MIS oscillations are also interesting owing to their interplay with another magneto-oscillatory phenomenon recently discovered in high-mobility 2D layers. If a 2D electron system is exposed to a continuous microwave (MW) irradiation, microwave-induced resistance oscillations (MIROs) occur, which are governed by the ratio of the radiation frequency ω to the cyclotron frequency ω_c.[8] With increasing radiation intensity, the minima of these oscillations evolve into "zero-resistance states"[9,10] in samples with ultrahigh electron mobility. Similar to MIS oscillations, MIROs originate from a periodic modulation of the probability of electron transitions between different Landau levels. In single-subband systems, such transitions occur because of electron scattering in the presence of microwave excitation, when electrons absorb radiation quanta and gain the energy necessary for the transitions. A detailed theoretical description of MIROs involves consideration of several microscopic mechanisms of photoresistance, which satisfactory describe the observed periodicity and phase of these oscillations.[11–14] Among them, the inelastic mechanism,[13] associated with a microwave-generated nonequilibrium oscillatory component of the isotropic part of the electron distribution function, dominates at low temperatures T, because its contribution is proportional to the inelastic relaxation time $\tau_{in} \propto T^{-2}$. Recently, MIROs have been studied in systems with two occupied subbands (DQWs).[15] It is found that the interplay between MIS oscillations and MIROs manifests itself as an interference of these kinds of oscillations, which is formally

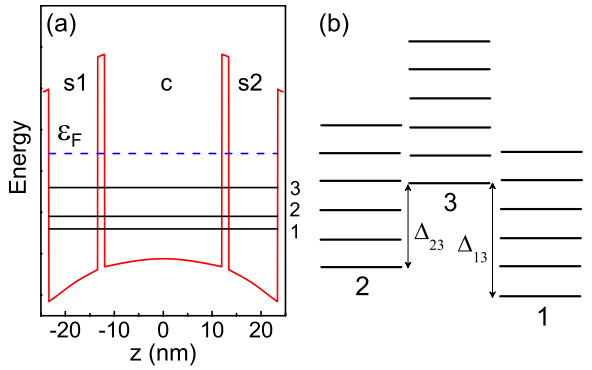

FIG. 1. (Color online) (a) Image of a triple quantum well and (b) Landau level staircase for a triple quantum well with three occupied subbands (1, 2, and 3).

expressed as a product of the corresponding oscillating factors.[15] The observed magnetoresistance pattern strongly depends on frequency ω and exhibits inversion or enhancement of certain groups of MIS peaks. It is established that the inelastic mechanism of microwave photoresistance explains magnetoresistance oscillations in such two-subband systems.[15]

Previous studies of MIS oscillations and their interference with MIROs have been restricted to two-subband systems. In this paper we present experimental and theoretical studies of these phenomena in systems with three occupied subbands formed in triple quantum wells (TQWs). The symmetric triple-well structure under investigation is shown in Fig. 1. The barriers dividing the wells are thin enough to have a strong tunnel hybridization of electron states in different wells. As a result, there exist three subbands with different quantization energies ε_j $(j=1,2,3)$ and all of them are occupied by electrons at the chosen (high enough) electron density. We have found that the magnetoresistance of such systems exhibits MIS oscillations with several periods determined by subband separation energies $\Delta_{jj'}=|\varepsilon_j-\varepsilon_{j'}|$. The peculiar MIS oscillation picture is distinct from that observed in DQWs, where only one MIS period exists. This feature has not been mentioned in previous studies of TQWs by other groups,[16,17] which concentrated on the regime of high magnetic fields and quantum Hall effect. Next, we have demonstrated that the MIS oscillation picture in TQWs exposed to microwave irradiation changes and depends on the radiation frequency. This behavior is basically similar to that in the case of DQWs described above. To explain the observed MIS oscillations and their interference with MIROs in TQWs, we generalize the magnetoresistance theory in the presence of microwave irradiation to the multisubband case. All experimental results are in agreement with theoretical calculations involving the inelastic mechanism of photoresistance.

The paper is organized as follows. Section II presents our experimental results for TQWs and a theoretical description of the MIS oscillations in many-subband systems. Section III presents the magnetoresistance under microwave irradiation, also together with a theoretical description, a comparison of theory and experiment, and a discussion of the results. Conclusions are given in the last section. Appendix A contains details of the theoretical calculation of photoresistance for many-subband systems and Appendix B describes the tight-binding approach for a calculation of subband spectrum and scattering rates in symmetric triple-well systems with application to our samples.

TABLE I. Subband separation energies for two samples, extracted from Fourier analysis of magnetoresistance.

Wafer	Δ_{12} (meV)	Δ_{23} (meV)	Δ_{13} (meV)
A	1.4	3.9	5.3
B	1.0	2.4	3.4

II. MIS OSCILLATIONS IN TRIPLE QUANTUM WELLS

Our samples are symmetrically doped GaAs TQWs, separated by $Al_xGa_{1-x}As$ barriers, with a high total electron sheet density of $n_s=9\times10^{11}$ cm^{-2} and mobilities of 5×10^5 cm^2/V s (wafer A) and 4×10^5 cm^2/V s (wafer B). The central well width is about 230 Å and both side wells have equal widths of 100 Å. The barrier thickness d_b is 14 Å (wafer A) and 20 Å (wafer B). In order to make the central well populated, we increased its width. The estimated density in the central well is 35% smaller than in the side wells. The layers are shunted by Ohmic contacts. Figure 1 gives an image of a triple quantum well with three occupied subbands $(j=1,2,3)$ and the staircases of Landau levels. The subband separation energies $\Delta_{jj'}$, which characterize the coupling strength between the quantum wells (see Appendix B), are presented in Table I. The measurements have been carried out in a dilution refrigerator (low-temperature MIS studies) and in a VTI cryostat using a waveguide for microwave experiments to deliver microwave radiation down to the sample. A conventional lock-in technique for magnetotransport measurements under a continuous microwave irradiation (35 to 170 GHz) has been used. Several specimens of both van der Pauw and Hall bar geometries from both wafers have been studied.

The description of the MIS oscillations will be focused on samples with $d_b=14$ Å owing to a stronger tunnel coupling which gives rise to better pronounced MIS features. In Fig. 2(a) we present temperature dependence of MIS oscillations from $T=1.4$ to 4.2 K. The inset also shows MIS oscillations at $T=50$ mK. For this low temperature and also at 1.4 K, the MIS oscillations are superimposed on low-field SdH oscillations. Figure 2(b) demonstrates MIS oscillations for both samples with $d_b=14$ Å and $d_b=20$ Å. It is obvious that for the thicker barrier, when tunnel coupling is weaker, the subband separation $\Delta_{jj'}$ becomes smaller and the probability of intersubband transitions of electrons decreases. This is reflected in the periodicity and in the amplitude of MIS oscillations (see also Table I).

To describe the data in more detail, we have generalized the theory of magnetoresistance in the systems with two occupied subbands (DQWs) (Refs. 6, 18, and 19) to the case of N subbands. We consider elastic scattering of electrons in the

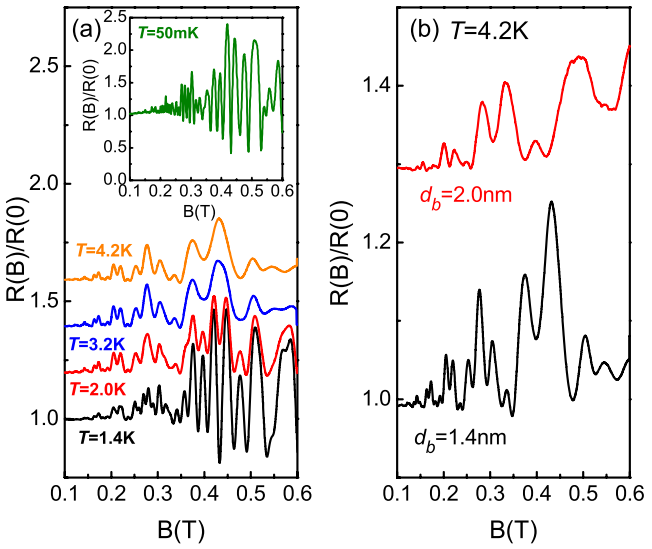

FIG. 2. (Color online) (a) Temperature dependence for MIS oscillations in a TQW with $d_b=14$ Å for 1.4, 2.0, 3.2, and 4.2 K. The inset shows MIS oscillations at 50 mK, superimposed on low-field SdH oscillations. (b) Comparison of both wafers with $d_b=20$ Å (top, shifted up for clarity) and $d_b=14$ Å (bottom) at $T=4.2$ K.

presence of a magnetic field under the condition of large filling factors (Fermi energy ε_F is much larger than $\hbar\omega_c$), and apply the self-consistent Born approximation to describe the density of states and the linear response. The expression for magnetoresistance is conveniently presented in the form

$$\rho_d = \rho_d^{(0)} + \rho_d^{(1)} + \rho_d^{(2)}, \tag{1}$$

where $\rho_d^{(0)}$ is the classical resistivity, $\rho_d^{(1)}$ is the first-order (linear in Dingle factors) quantum contribution describing the SdH oscillations, and $\rho_d^{(2)}$ is the second-order (quadratic in Dingle factors) quantum contribution containing the MIS oscillations. In the regime of classically strong magnetic fields, one obtains

$$\rho_d^{(0)} = \frac{m}{e^2 n_s \tau_{tr}}, \quad \frac{1}{\tau_{tr}} = \frac{1}{N}\sum_j \nu_j^{tr}, \tag{2}$$

$$\rho_d^{(1)} = -\mathcal{T}\frac{4m}{e^2 n_s}\frac{1}{N}\sum_j \nu_j^{tr} d_j \cos\frac{2\pi(\varepsilon_F - \varepsilon_j)}{\hbar\omega_c}, \tag{3}$$

and

$$\rho_d^{(2)} = \frac{m}{e^2 n_s}\sum_{jj'}\frac{n_j + n_{j'}}{n_s}\nu_{jj'}^{tr} d_j d_{j'} \cos\frac{2\pi\Delta_{jj'}}{\hbar\omega_c}, \tag{4}$$

where m is the effective mass of electrons, $d_j=\exp(-\pi\nu_j/\omega_c)$ are the Dingle factors, $\mathcal{T}=X/\sinh X$ with $X=2\pi^2 T/\hbar\omega_c$ is the thermal suppression factor, and n_j are the partial densities in the subbands ($\Sigma_j n_j = n_s$). The sums are taken over all subbands, and since for the terms with $j=j'$ one has $\Delta_{jj'}=0$, the corresponding cosines in Eq. (4) are equal to 1. The subband-dependent quantum relaxation rates ν_j and $\nu_{jj'}$ as well as the transport scattering rates ν_j^{tr} and $\nu_{jj'}^{tr}$ entering Eqs. (2)–(4) are defined according to

$$\nu_j = \sum_{j'} \nu_{jj'}, \quad \nu_j^{tr} = N\sum_{j'}\frac{n_j + n_{j'}}{2n_s}\nu_{jj'}^{tr}, \tag{5}$$

and

$$\left.\begin{matrix}\nu_{jj'} \\ \nu_{jj'}^{tr}\end{matrix}\right\} = \int_0^{2\pi}\frac{d\theta}{2\pi}\nu_{jj'}(\theta)\left\{\begin{matrix}1 \\ F_{jj'}(\theta)\end{matrix}\right. ,$$

$$\nu_{jj'}(\theta) = \frac{m}{\hbar^3} w_{jj'}(\sqrt{(k_j^2 + k_{j'}^2)F_{jj'}(\theta)}), \tag{6}$$

where $w_{jj'}(q)$ are the Fourier transforms of the correlators of the scattering potential, $F_{jj'}(\theta)=1-2k_j k_{j'}\cos\theta/(k_j^2+k_{j'}^2)$, θ is the scattering angle, and $k_j=\sqrt{2\pi n_j}$ is the Fermi wave number for subband j. Since $F_{jj}=1-\cos\theta$, the intrasubband transport rates ν_{jj}^{tr} are defined in a conventional way. The theory is valid if the subband separations $\Delta_{jj'}$ are large compared to the broadening energies $\hbar\nu_j$ and the Dingle factors are small, $d_j^2 \ll 1$. In a similar way as we introduced the averaged transport time τ_{tr} by Eq. (2), one can introduce the averaged quantum lifetime $1/\tau_q = N^{-1}\Sigma_j \nu_j$. Application of Eqs. (1)–(6) to the particular case of three subbands ($N=3, j=1,2,3$) is straightforward.

The behavior of magnetoresistance can be illustrated within a simple model using equal electron densities $n_j = n_s/N$ and assuming that all $\nu_{jj'}^{tr}$ and d_j are equal to each other, in particular, $d_j=d=\exp(-\pi/\omega_c\tau_q)$. Neglecting the SdH oscillations, we obtain for $N=3$

$$\frac{\rho_d(B)}{\rho_d(0)} \simeq 1 + \frac{2}{3}d^2\left[1 + \frac{2}{3}\cos\left(\frac{2\pi\Delta_{12}}{\hbar\omega_c}\right) + \frac{2}{3}\cos\left(\frac{2\pi\Delta_{13}}{\hbar\omega_c}\right) + \frac{2}{3}\cos\left(\frac{2\pi\Delta_{23}}{\hbar\omega_c}\right)\right]. \tag{7}$$

The MIS oscillations are represented as a superposition of three oscillating terms determined by relative positions of the subband energies. Notice that this expression does not depend on transport rates except the one standing in the Dingle factor d. The approximation in Eq. (7), in principle, can be applied for estimates to our system, since we have high total electron-sheet density and a strong tunnel coupling. To describe experimental magnetoresistance in detail, a more careful calculation based on Eqs. (1)–(6) is required.

We calculate the magnetoresistance of our system under a simplified assumption that the scattering potential is essential only in the side (s) wells, since the growth technology implies that most of the scatterers reside in the outer barriers. The correlation length $l_c=18.3$ nm entering the scattering potential correlator $w_{jj'}(q) \propto w_s(q)$ (see Appendix B for details) is determined by comparing the results of calculations to low-temperature magnetoresistance data for the samples with mobility 5×10^5 cm^2/V s. The averaged quantum lifetime estimated in this way is $\tau_q \simeq 3.8$ ps. The experiment shows a slow suppression of the MIS oscillations with temperature, which occurs owing to the contribution of electron-electron scattering into Landau-level broadening. Though the

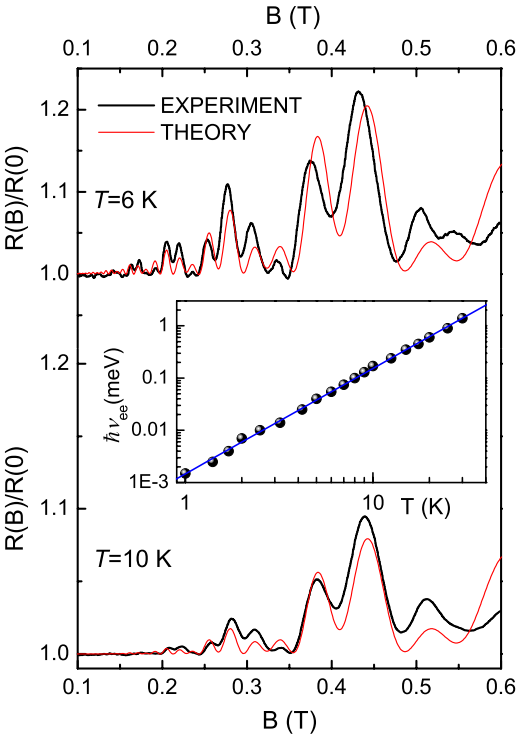

FIG. 3. (Color online) Comparison of the experimental and theoretical traces for a TQW with $d_b=14$ Å at $T=6$ K (top) and $T=10$ K (bottom). By fitting the amplitude of MIS oscillations, electron-electron scattering rate ν_{ee} is extracted (see the points in the inset). The linear fit to experimental data (line) corresponds to the theoretical dependence of Eq. (8) with $\lambda=2.2$.

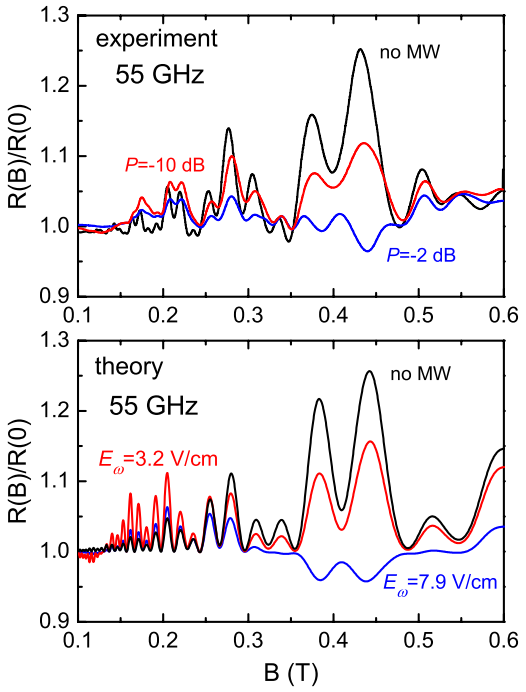

FIG. 4. (Color online) Measured (upper panel) and calculated (lower panel) magnetoresistance for TQW with $d_b=14$ Å at a lattice temperature of $T=4.2$ K under excitation by microwaves with a frequency of 55 GHz. The microwave electric field E_ω used for calculation of the magnetoresistance (see details in the text) corresponds to a different microwave power in decibel.

theory presented above does not take this effect into account explicitly, it can be improved by replacing the quantum relaxation rates according to

$$\nu_j \to \nu_j + \nu_{ee}, \quad \nu_{ee} = \lambda \frac{T^2}{\hbar \varepsilon_F}, \tag{8}$$

where ν_{ee} is the electron-electron scattering rate,[20,21] the Fermi energy is expressed through the averaged electron density as $\varepsilon_F=\hbar^2\pi(n_s/3)/m$, and λ is a numerical constant of order unity. In Fig. 3 we present a comparison of experiment and theory for two chosen temperatures, $T=6$ and 10 K. We have carried out this procedure for many temperatures from $T=1$ K up to 30 K, and estimated ν_{ee} by fitting the amplitudes of theoretical and experimental magnetoresistance traces. The effect of electron-electron scattering becomes essential for $T>2$ K and strongly reduces the amplitude of the MIS oscillations at $T\sim 10$ K. As seen from the log-log plot in the inset to Fig. 3, the extracted scattering rate ν_{ee} follows the T^2 dependence, in accordance with Eq. (8). This behavior is similar to that observed in DQWs.[6] Using $\varepsilon_F \simeq 10.5$ meV, we find $\lambda=2.2$.

III. INFLUENCE OF MICROWAVES ON MIS OSCILLATIONS

In this section, we investigate the influence of a continuous microwave irradiation on our TQW system. We have studied power, temperature, and frequency dependence of magnetoresistance for both wafers, though we focus again on the samples with $d_b=14$ Å.

In the upper part of Fig. 4 we present the magnetoresistance for different microwave powers at a temperature of $T=4.2$ K and a frequency of 55 GHz. Without microwave irradiation (no MW) only the MIS oscillations are visible. An increase in microwave power (−10 dB attenuation) leads to an enhancement of all MIS features for $B<0.25$ T and to a damping of all such features for $B>0.35$ T whereas the MIS oscillations around $B=0.3$ T are almost unchanged. A further increase in power (−2 dB attenuation) leads to a damping of the MIS oscillation amplitude for $B<0.25$ T, slightly increased compared to the MIS oscillation amplitude without microwave irradiation. The MIS features around $B=0.3$ T are considerably damped, while for $0.35<B<0.5$ T the MIS peaks are inverted. No polarization dependence of magnetoresistance has been found.

A similar behavior, with enhanced, suppressed, or inverted MIS peaks is observed in the magnetoresistance measured at different microwave frequencies in the range between 35 and 170 GHz, as shown in the upper part of Fig. 5. A strongly modified picture of the MIS oscillations correlates with the microwave frequency. The features most affected by the microwave irradiation, strongly sensitive to its frequency, occur at $B=0.27$ and 0.43 T. The plots for 110 and 170 GHz definitely show several regions of enhanced peaks and two regions of suppressed or inverted peaks (for example, the regions around 0.18 and 0.34 T for 170 GHz). For 35 GHz,

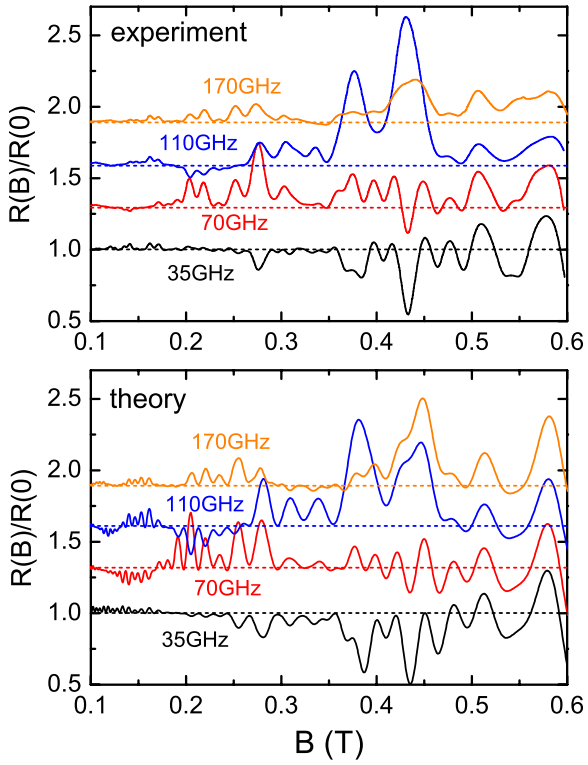

FIG. 5. (Color online) Measured (upper panel) and calculated (lower panel) magnetoresistances for a TQW with $d_b=14$ Å at the lattice temperature $T=1.4$ K for several chosen frequencies. The curves for 70, 110, and 170 GHz are shifted up for clarity.

all the MIS oscillations above 0.2 T are inverted. For 35 and 70 GHz, some SdH oscillations are visible in the region above 0.4 T. For 110 and 170 GHz, when the absorption of microwave radiation in this region is higher, the SdH oscillations are suppressed because of the heating of the electron gas by microwaves.

The peculiar features of the microwave-modified magnetoresistance can be understood in terms of interference of the MIS oscillations with MIROs. This phenomenon is already known for two-subband systems.[15] The theory applied for explanation of our measurements is presented below. The dissipative resistivity in the presence of microwaves is given by (see Appendix A for derivation of the expressions)

$$\rho_d^{\mathrm{MW}} = \rho_d + \rho_{in} + \rho_{di}, \tag{9}$$

where the dark resistivity ρ_d is described in Sec. II, while ρ_{in} and ρ_{di} are the microwave-induced contributions due to inelastic and displacement mechanisms, respectively. At low temperatures ρ_{in} is the main contribution. It is given by

$$\rho_{in} = -\frac{m}{e^2 n_s}\frac{2\tau_{tr}A_\omega}{N^2}\sum_{jj'}\nu_j^{tr}\nu_{j'}^{tr}d_j d_{j'}\cos\frac{2\pi\Delta_{jj'}}{\hbar\omega_c}, \tag{10}$$

where

$$A_\omega = \frac{\mathcal{P}_\omega(2\pi\omega/\omega_c)\sin(2\pi\omega/\omega_c)}{1+\mathcal{P}_\omega\sin^2(\pi\omega/\omega_c)} \tag{11}$$

is an oscillating function describing MIROs and

$$\mathcal{P}_\omega = \frac{\tau_{in}}{\tau_{tr}}P_\omega, \quad P_\omega = \left(\frac{eE_\omega}{\hbar\omega}\right)^2\overline{v_F^2}(|s_+|^2+|s_-|^2) \tag{12}$$

is the dimensionless function proportional to the microwave power. In this expression, $\overline{v_F^2}=N^{-1}\Sigma_j v_j^2$ is the averaged Fermi velocity and τ_{in} is the averaged inelastic relaxation time introduced in Appendix A. The averaged transport time τ_{tr} is defined in Sec. II and the coefficients $s_\pm$ are given in Appendix A. Notice that in the case of linear polarization of radiation, and away from the cyclotron resonance, $|s_+|^2+|s_-|^2 \simeq (\omega^2+\omega_c^2)/(\omega^2-\omega_c^2)^2$. The contribution ρ_{di} is presented in Appendix A. Since ρ_{di} is much smaller than ρ_{in}, it is not taken into account in our consideration. The influence of microwave radiation on the SdH oscillations can also be neglected at weak radiation power.

To get a visual description of the influence of radiation on magnetoresistance, we again use a simple model assuming equal partial densities $n_j=n_s/N$, equal transport scattering rates $\nu_{jj'}^{tr}$, and Dingle factors $d_j=d$. The magnetoresistance of three-subband system ($N=3$) then takes the form

$$\frac{\rho_d^{\mathrm{MW}}(B)}{\rho_d(0)} \simeq 1+\frac{2}{3}(1-A_\omega)d^2\left[1+\frac{2}{3}\cos\left(\frac{2\pi\Delta_{12}}{\hbar\omega_c}\right)+\frac{2}{3}\cos\left(\frac{2\pi\Delta_{13}}{\hbar\omega_c}\right)+\frac{2}{3}\cos\left(\frac{2\pi\Delta_{23}}{\hbar\omega_c}\right)\right], \tag{13}$$

which differs from Eq. (7) only by the presence of the factor $1-A_\omega$. The products of A_ω by the MIS oscillation factors $\cos(2\pi\Delta_{jj'}/\hbar\omega_c)$ lead to interference oscillations of the magnetoresistance. In the regions of frequency where A_ω is negative, one expects an enhancement of the MIS peaks. If A_ω is positive, the peaks are suppressed and inverted with increasing microwave power. This is the main feature of the behavior we observe experimentally in Figs. 4 and 5.

A comparison of experimental results with theory based on Eqs. (10)–(12) is demonstrated in the lower parts of Figs. 4 and 5. Apart from the known parameters used also in Sec. II, we apply the following estimate for the inelastic relaxation time:[13] $\tau_{in}\simeq\hbar\varepsilon_F/T^2$, assuming that the relaxation is governed by the electron-electron interaction. The reliability of this estimate is confirmed in numerous experiments on magnetoresistance influenced by either microwave field[15,22] or static electric field.[23,24] To explain the experimental data, it is important to take into account microwave heating of the electron gas. This effect is directly visible in our experiment and results in a suppression of the SdH oscillations under microwave irradiation. The increase in the effective electron temperature over the lattice temperature also leads to a decrease in the inelastic relaxation time and quantum lifetimes, see Eq. (8), so the MIS oscillation amplitudes are expected to be suppressed as a result of electron heating. The electron temperature, which depends on the magnetic field, radiation frequency, and power, has been calculated assuming energy relaxation of electrons due to their interaction with acoustic phonons. Finally, to determine the electric field E_ω corresponding to our measurements, we use an estimate for the microwave electric field generated by our source as 10 V/cm (at 55 GHz). Thus, the attenuations of −10 and −2 dB cor-

respond to E_ω=3.2 and 7.9 V/cm, respectively, and we applied these values for calculation of the magnetoresistance shown in Fig. 4.

The theoretical plots in Fig. 4 reproduce all the basic features of the experimental magnetoresistance traces, in particular, a suppression and inversion of two MIS peaks around B=0.4 T, because of the contribution ρ_{in} with positive A_ω. Notice that the nonmonotonic power dependence of the MIS peaks around 0.2 T is explained by the interplay of MIS/MIRO interference and heating effects. At low radiation power the enhancement of these peaks occurs because of the contribution ρ_{in} with negative A_ω. At high power, when the saturation effect takes place,[13,14] a decrease in the Dingle factors due to the heating-induced increase in ν_{ee} becomes more important and the MIS peaks are suppressed.

The expected microwave electric field in the frequency-dependent measurements shown in Fig. 5 is $E_\omega \sim 3$ V/cm. To get a closer resemblance of the theoretical magnetoresistance to the experimental plots, we slightly varied E_ω around this value and obtained the best fit at E_ω=3.5 V/cm for 35 and 70 GHz, 4 V/cm for 110 GHz, and 2.2 V/cm for 170 GHz. The corresponding theoretical plots are presented in Fig. 5. Since the lattice temperature for these measurements is 1.4 K, the heating effect appears to be considerable. For 35, 70, and 110 GHz, the calculated electron temperature in the vicinity of the cyclotron resonance is about 3.5 K, which is close to our experimental estimates obtained from suppression of the SdH oscillations. In general, a reasonably good agreement between theory and experiment at different frequencies suggests that the theoretical model applied for the calculations is reliable.

IV. CONCLUSIONS

We have studied transport properties, including microwave photoresistance, of the electron systems with three occupied 2D subbands in perpendicular magnetic fields. Such systems are realized in TQWs with high enough electron density. As we have demonstrated, both experimentally and theoretically, the magnetoresistance of TQWs is qualitatively different from that for single-subband and two-subband systems, and contains a superposition of three oscillating terms whose frequencies are given by the subband separation energies Δ_{12}, Δ_{13}, and Δ_{23}. This occurs because the quantum contribution to the resistivity is essentially determined by electron scattering between the Landau levels of different subbands. Therefore, there exist MIS oscillations of resistivity, and the picture of these oscillations becomes complicated in the systems with more than two occupied subbands. We have presented a theoretical description of such oscillations by generalizing the theory of quantum magnetoresistance to the multisubband case and obtained a good agreement with the experiment.

Similar as in single-subband and two-subband systems, the quantum contribution to the resistivity decreases with increasing temperature T because of the decrease in quantum lifetime due to enhanced contribution of electron-electron scattering. By measuring the amplitude of the MIS oscillations at different temperatures up to 30 K, we have established that the temperature dependence of electron-electron scattering rate follows the theoretically predicted T^2 law, see Eq. (8). The numerical constant λ in this dependence, λ=2.2, is close enough to those determined from the MIS oscillations in two-subband systems, both in double quantum wells[6] (λ=3.5) and in single quantum wells[25] (λ=2.6). Therefore, one may conclude that the influence of electron-electron scattering on the quantum lifetime of electrons is not very sensitive to the number of occupied subbands.

The TQWs exposed to a continuous microwave irradiation demonstrate dramatic changes in magnetoresistance. The effect of microwaves is understood as a result of interference of MIS oscillations and microwave-induced resistance oscillations. A similar effect takes place for two-subband systems in double quantum wells,[15] where it is easier recognizable owing to a simpler picture of the MIS oscillations. To describe our observations, we have developed a theory of magnetoresistance of multisubband systems under microwave irradiation, and applied it to our three-subband systems. Among the mechanisms of microwave photoresistance, the inelastic mechanism is found to be responsible for the observed magnetoresistance features. In spite of several approximations of the theory, in particular, those for description of elastic scattering (see Appendix B), we have obtained a good agreement between theoretical and experimental magnetoresistance traces by using an established estimate for the inelastic relaxation time.

In summary, our investigation of low-field magnetotransport in three-subband systems both with and without microwave excitation is a useful step toward understanding the influence of energy spectrum and scattering mechanisms on the transport properties of low-dimensional electrons.

ACKNOWLEDGMENTS

The authors thank M. A. Zudov, I. A. Dmitriev, S. Vitkalov, and S. A. Studenikin for helpful discussions. This work was supported by COFECUB-USP (Project No. U$_c$109/08), CNPq, FAPESP, and with microwave facilities from ANR MICONANO.

APPENDIX A: MICROWAVE PHOTORESISTANCE OF A MANY-SUBBAND SYSTEM

In the presence of electromagnetic radiation (microwaves) of frequency ω and under a dc excitation, one can derive the quantum Boltzmann equation for electrons in a magnetic field by using a transition to the moving coordinate frame, in a similar way as for the single-subband system (see Ref. 14 and references therein). This leads to the kinetic equation for the Wigner distribution function $f_{j\varepsilon\varphi}$, which depends on the subband index j, energy ε, and angle φ of the electron momentum

$$\omega_c \frac{\partial f_{j\varepsilon\varphi}}{\partial \varphi} = \sum_{j'} \int_0^{2\pi} \frac{d\varphi'}{2\pi} \nu_{jj'}(\varphi - \varphi') \sum_n [J_n(\beta_{jj'})]^2 \times D_{j'}(\varepsilon + n\omega + \gamma_{jj'})[f_{j',\varepsilon+n\omega+\gamma_{jj'},\varphi'} - f_{j\varepsilon\varphi}] + J_{in}. \quad \text{(A1)}$$

Notice that in this appendix we use the system of units where

$\hbar=1$. In the kinetic equation, we introduced the dimensionless (normalized to its zero-field value) density of states $D_j(\varepsilon)$. Next, $J_n(x)$ is the Bessel function, J_{in} is the collision integral describing inelastic scattering, and $\nu_{jj'}$ are the scattering rates defined in Sec. II. The other quantities standing in Eq. (A1) are

$$\beta_{jj'}(\varphi,\varphi') = \frac{eE_\omega}{\sqrt{2}\omega}|s_-(v_j e^{i\varphi} - v_{j'}e^{i\varphi'}) + s_+(v_j e^{-i\varphi} - v_{j'}e^{-i\varphi'})| \tag{A2}$$

and

$$\gamma_{jj'}(\varphi,\varphi') = \frac{e}{2i\omega_c}[E_-(v_j e^{i\varphi} - v_{j'}e^{i\varphi'}) - E_+(v_j e^{-i\varphi} - v_{j'}e^{-i\varphi'})], \tag{A3}$$

where $E_\pm = E_x \pm iE_y$, $\mathbf{E}=(E_x,E_y)$ is the dc field strength, E_ω is the strength of microwave electric field (related to the incident microwave field strength E_i in vacuum as $E_\omega = E_i/\sqrt{\epsilon^*}$, see below), and $v_j = p_j/m$ are the subband-dependent Fermi velocities. The factors $s_\pm$ describe polarization of the radiation and account for electrodynamic effects.[26,27] For the case of linear polarization,

$$s_\pm = \frac{1}{\sqrt{2}}\frac{1}{\omega \pm \omega_c + i\omega_p}, \tag{A4}$$

where $\omega_p = 2\pi e^2 n_s/mc\sqrt{\epsilon^*}$, $\sqrt{\epsilon^*}=(\sqrt{\epsilon_{vac}}+\sqrt{\epsilon_d})/2$, $\epsilon_{vac}=1$ is the dielectric permittivity of vacuum, and ϵ_d is the dielectric permittivity of the medium surrounding the quantum wells.

The distribution function can be expanded in the angular harmonics: $f_{j\varepsilon\varphi}=\Sigma_l f_{j\varepsilon l}e^{il\varphi}$. The density of dissipative electric current in the 2D plane, $\mathbf{j}=(j_x,j_y)$, is determined by the $l=1$ harmonic

$$j_- \equiv j_x - ij_y = \frac{e}{\pi}\sum_j p_j \int d\varepsilon D_j(\varepsilon) f_{j\varepsilon 1}. \tag{A5}$$

In the regime of classically strong magnetic fields, the anisotropic part of the distribution function is expressed through the isotropic (angular-independent) part $f_{j\varepsilon}\equiv f_{j\varepsilon l}$ for $l=0$. This leads to the expression for the current in the form

$$j_- = \frac{e}{i\pi\omega_c}\sum_{jj'} p_j \int d\varepsilon D_j(\varepsilon)\int_0^{2\pi}\frac{d\varphi}{2\pi}e^{-i\varphi}\int_0^{2\pi}\frac{d\varphi'}{2\pi} \times \nu_{jj'}(\varphi-\varphi')\sum_n [J_n(\beta_{jj'})]^2 D_{j'}(\varepsilon+n\omega+\gamma_{jj'}) \times [f_{j'\varepsilon+n\omega+\gamma_{jj'}} - f_{j\varepsilon}]. \tag{A6}$$

The response to $E_-[j_-=\sigma_d E_-]$ gives the symmetric part of dissipative conductivity considered below. The resistivity is then given by $\rho_d^{\mathrm{MW}}=\sigma_d/\sigma_\perp^2$, where $\sigma_\perp = e^2 n_s/m\omega_c$ is the classical Hall conductivity.

The isotropic part of the distribution function can be represented in the form

$$f_{j\varepsilon} = f_\varepsilon^{(0)} - i\omega\frac{\partial f_\varepsilon^{(0)}}{\partial\varepsilon}g_{j\varepsilon}, \tag{A7}$$

where $f_\varepsilon^{(0)}$ is a slowly varying function of energy, which is close to a quasiequilibrium (heated Fermi) distribution, while $g_{j\varepsilon}$ is a rapidly oscillating (periodic in $\hbar\omega_c$) function, which is also represented as $g_{j\varepsilon}=\Sigma_k g_{jk}\exp(2\pi ik\varepsilon/\omega_c)$. After a substitution of expression (A7) into Eq. (A6), the contribution coming from $f_\varepsilon^{(0)}$ produces the "dark" resistivity and its modification by the microwaves due to displacement mechanism. The microwave modification of the resistivity due to the inelastic mechanism originates from the term proportional to $g_{j\varepsilon}$. In the following, we search for the response linear in the dc field and quadratic in the microwave field. This is done by expanding the Bessel functions in powers of $\beta_{jj'}$ and retaining only the lowest-order terms. Also, we use the lowest-order expansion of the density of states in the Dingle factors, $D_j(\varepsilon)\simeq 1-2d_j\cos[2\pi(\varepsilon-\varepsilon_j)/\omega_c]$, so only the lowest oscillatory harmonics ($k=\pm 1$) are relevant. The angular and energy averaging in Eq. (A6) in this case are carried out analytically, and one gets the expression for the dark resistivity ρ_d (Sec. II), as well as the microwave-induced contributions ρ_{di} and ρ_{in}

$$\rho_{di} = -\frac{m}{e^2 n_s}P_\omega\left[\sin^2\frac{\pi\omega}{\omega_c} + \frac{\pi\omega}{\omega_c}\sin\frac{2\pi\omega}{\omega_c}\right] \times \frac{N}{2}\sum_{jj'}\left(\frac{n_j+n_{j'}}{n_s}\right)^2 \nu_{jj'}^* d_j d_{j'}\cos\frac{2\pi\Delta_{jj'}}{\omega_c}, \tag{A8}$$

where P_ω is defined by Eq. (12),

$$\nu_{jj'}^* = \int_0^{2\pi}\frac{d\theta}{2\pi}\nu_{jj'}(\theta)[F_{jj'}(\theta)]^2 \tag{A9}$$

and

$$\rho_{in} = -\frac{m}{e^2 n_s}\frac{2\pi\omega}{\omega_c}\sum_{jj'}\frac{n_j+n_{j'}}{n_s}\nu_{jj'}^{tr} \times\left[g_{j'1}d_j\exp\left(\frac{2\pi i\varepsilon_j}{\omega_c}\right) + \text{c.c.}\right]. \tag{A10}$$

One can find $g_{j\varepsilon}$ from the isotropic part of Eq. (A1) by using the relaxation time approximation for the isotropic part of the inelastic collision integral

$$J_{in} = -\frac{f_{j\varepsilon} - f_\varepsilon^{(0)}}{\tau_j^{in}}. \tag{A11}$$

This approximation is valid for small deviations $f_{j\varepsilon}-f_\varepsilon^{(0)}$, and is justified in a similar way as for the single-subband systems, based on a linearization of the collision integral for electron-electron scattering.[13] After substitution of expression (A11) into Eq. (A1), one can obtain a system of linear equations for g_{jk}, which is easily solved under a reasonable condition that the intersubband scattering dominates over the inelastic one: $\nu_{jj'} \gg 1/\tau_j^{in}$ $(j\neq j')$. This gives subband-independent harmonics $g_{jk}=g_k$, in particular,

$$g_1 = \frac{P_\omega \tau_{in} \sin(2\pi\omega/\omega_c)}{1 + P_\omega(\tau_{in}/\tau_{tr})\sin^2(\pi\omega/\omega_c)} \times \frac{1}{2N}\sum_j \nu_j^{tr} d_j \exp\left(-\frac{2\pi i \varepsilon_j}{\omega_c}\right), \quad \text{(A12)}$$

where the averaged inelastic relaxation time is defined according to $1/\tau_{in} = N^{-1}\Sigma_j 1/\tau_j^{in}$. The denominator in Eq. (A12) describes the effect of saturation. A substitution of the result Eq. (A12) into Eq. (A10) leads to Eq. (10).

APPENDIX B: ELECTRON SPECTRUM AND SCATTERING RATES IN A TRIPLE-WELL SYSTEM

To describe the scattering rates, we employ the wave functions and electron energies in the subbands found from the tight-binding Hamiltonian[28] using the expansion of the wave function $\psi(z) = \Sigma_i \varphi_i F_i(z)$ in the basis of single-well orbitals $F_i(z)$ ($i = 1,2,3$ numbers the left, central, and right well, respectively). This leads to the matrix equation for the coefficients φ_i

$$\begin{pmatrix} \varepsilon_1^{(0)} - \varepsilon & -t_{12} & 0 \\ -t_{12} & \varepsilon_2^{(0)} - \varepsilon & -t_{23} \\ 0 & -t_{23} & \varepsilon_3^{(0)} - \varepsilon \end{pmatrix} \begin{pmatrix} \varphi_1 \\ \varphi_2 \\ \varphi_3 \end{pmatrix} = 0, \quad \text{(B1)}$$

where $\varepsilon_i^{(0)}$ are the single-well quantization energies and $t_{ii'}$ are the tunneling amplitudes. For the case of symmetric TQWs ($\varepsilon_1^{(0)} = \varepsilon_3^{(0)} \equiv \varepsilon_s, \varepsilon_2^{(0)} \equiv \varepsilon_c, t_{12} = t_{23} \equiv t$) the energies of the three subbands, ε_j, are[28]

$$\varepsilon_1 = (\varepsilon_c + \varepsilon_s)/2 - \Lambda,$$

$$\varepsilon_2 = \varepsilon_s,$$

$$\varepsilon_3 = (\varepsilon_c + \varepsilon_s)/2 + \Lambda,$$

$$\Lambda = \sqrt{(\varepsilon_c - \varepsilon_s)^2/4 + 2t^2}. \quad \text{(B2)}$$

The corresponding eigenstates are expressed through the single-well orbitals as $\psi_j(z) = \Sigma_i \chi_{ij} F_i(z)$. The matrix χ_{ij} is given by

$$\chi_{ij} = \begin{pmatrix} C_1 t/(\varepsilon_s - \varepsilon_1) & 1/\sqrt{2} & C_3 t/(\varepsilon_s - \varepsilon_3) \\ C_1 & 0 & C_3 \\ C_1 t/(\varepsilon_s - \varepsilon_1) & -1/\sqrt{2} & C_3 t/(\varepsilon_s - \varepsilon_3) \end{pmatrix}, \quad \text{(B3)}$$

where $C_{1,3} = [1 + 2t^2/(\varepsilon_s - \varepsilon_{1,3})^2]^{-1/2}$. This matrix is composed from the three columns of φ_i for the states $j = 1,2,3$.

The parameters of the tight-binding model can be extracted from the subband gaps found experimentally. By setting ε_s as the reference energy, one has

$$\varepsilon_c = \Delta_{23} - \Delta_{12}, \quad t = \sqrt{\Delta_{23}\Delta_{12}/2}. \quad \text{(B4)}$$

For our samples (wafer A) we obtain $\varepsilon_c = 2.5$ meV and $2t = 3.35$ meV. Using the total density $n_s = 9 \times 10^{11}$ cm^{-2}, one can find the subband densities $n_1 = 3.62 \times 10^{11}$ cm^{-2}, $n_2 = 3.23 \times 10^{11}$ cm^{-2}, and $n_3 = 2.14 \times 10^{11}$ cm^{-2}. The electron density in each side well is $n_{side} = \Sigma_j \chi_{1j}^2 n_j = \Sigma_j \chi_{3j}^2 n_j = 3.23 \times 10^{11}$ cm^{-2} and the electron density in the central well is $n_{cent} = \Sigma_j \chi_{2j}^2 n_j = 2.53 \times 10^{11}$ cm^{-2}.

The random scattering potential acting on electrons is $V(\mathbf{r}, z)$, where $\mathbf{r}$ is the in-plane coordinate vector and z is the coordinate in the growth direction. The matrix elements of this potential, $V_{jj'}(\mathbf{r})$, are expressed through the effective 2D potentials in the layers, introduced as $V_i(\mathbf{r}) = \int dz |F_i(z)|^2 V(\mathbf{r}, z)$. Accordingly, the correlators of the potentials are written through the correlators of $V_i(\mathbf{r})$

$$W_{jj'}(|\mathbf{r} - \mathbf{r}'|) \equiv \langle\langle V_{jj'}(\mathbf{r}) V_{j'j}(\mathbf{r}')\rangle\rangle = \sum_{ii'} \chi_{ij}\chi_{ij'}\chi_{i'j'}\chi_{i'j}\tilde{W}_{ii'}(|\mathbf{r} - \mathbf{r}'|). \quad \text{(B5)}$$

The product of the factors χ determines the overlap of the electron wave functions, while the factors $\tilde{W}_{ii'}(|\mathbf{r} - \mathbf{r}'|) \equiv \langle\langle V_i(\mathbf{r}) V_{i'}(\mathbf{r}')\rangle\rangle$ describe intralayer $i = i'$ and interlayer $i \neq i'$ potential correlations. In TQWs one can neglect interlayer correlations between the potentials of the side wells because of a large distance between these wells: $\tilde{W}_{13} \simeq 0$. Then, symmetric TQWs are characterized by three correlators: $W_s = \tilde{W}_{11} = \tilde{W}_{33}$, $W_c = \tilde{W}_{22}$, and $W_{sc} = \tilde{W}_{12} = \tilde{W}_{23} = \tilde{W}_{21} = \tilde{W}_{32}$. A reasonable approximation for our TQWs is to assume that the effective potential in the central well, $V_2(\mathbf{r})$, is much weaker than the side-well potentials. In this case, W_c and W_{sc} can be neglected compared to W_s, and Eq. (B5) is rewritten as

$$W_{jj'}(|\mathbf{r} - \mathbf{r}'|) \simeq 2\chi_{1j}^2 \chi_{1j'}^2 W_s(|\mathbf{r} - \mathbf{r}'|). \quad \text{(B6)}$$

The spatial Fourier transform $w_{jj'}(q) = \int d\mathbf{r} \exp(-i\mathbf{q}\cdot\mathbf{r}) W_{jj'}(|\mathbf{r}|)$ determines all scattering rates according to Eqs. (5) and (6). In the approximation Eq. (B6), $w_{jj'}(q) \simeq \chi_{1j}^2 \chi_{1j'}^2 w_s(q)$, where $w_s(q)$ is the spatial Fourier transform of W_s. The concrete form of the function $w_s(q)$ depends on the nature of the scatterers, their distribution in the structure, and on the TQW potential, which determines the shape of $F_i(z)$. In the case of long-range scattering potential, the magnetoresistance $\rho_d(B)/\rho_d(0)$ is weakly sensitive to this form, but essentially depends on the effective correlation length l_c which defines the scale of the q dependence. In our calculations, we use a model $w_s(q) \propto \exp(-l_c q)$.

[1] D. Schoenberg, *Magnetic Oscillations in Metals* (Cambridge University Press, Cambridge, 1984).
[2] V. Polyanovsky, Fiz. Tekh. Poluprovodn. **22**, 2230 (1988) [Sov. Phys. Semicond. **22**, 1408 (1988)].
[3] D. R. Leadley, R. Fletcher, R. J. Nicholas, F. Tao, C. T. Foxon, and J. J. Harris, Phys. Rev. B **46**, 12439 (1992).
[4] T. H. Sander, S. N. Holmes, J. J. Harris, D. K. Maude, and J. C. Portal, Phys. Rev. B **58**, 13856 (1998).
[5] A. C. H. Rowe, J. Nehls, R. A. Stradling, and R. S. Ferguson, Phys. Rev. B **63**, 201307(R) (2001).
[6] N. C. Mamani, G. M. Gusev, T. E. Lamas, A. K. Bakarov, and O. E. Raichev, Phys. Rev. B **77**, 205327 (2008).
[7] A. A. Bykov, D. P. Islamov, A. V. Goran, and A. I. Toropov, JETP Lett. **87**, 477 (2008).
[8] M. A. Zudov, R. R. Du, J. A. Simmons, and J. L. Reno, Phys. Rev. B **64**, 201311(R) (2001).
[9] R. G. Mani, J. H. Smet, K. von Klitzing, V. Narayanamurti, W. B. Johnson, and V. Umansky, Nature (London) **420**, 646 (2002).
[10] M. A. Zudov, R. R. Du, L. N. Pfeiffer, and K. W. West, Phys. Rev. Lett. **90**, 046807 (2003).
[11] V. I. Ryzhii, Fiz. Tverd. Tela (Leningrad) **11**, 2577 (1969) [Sov. Phys. Solid State **11**, 2078 (1970)]; V. I. Ryzhii, R. A. Surris, and B. S. Shchamkhalova, Fiz. Tekh. Poluprovodn. **20**, 2078 (1986) [Sov. Phys. Semicond. **20**, 1299 (1986)].
[12] A. C. Durst, S. Sachdev, N. Read, and S. M. Girvin, Phys. Rev. Lett. **91**, 086803 (2003).
[13] I. A. Dmitriev, M. G. Vavilov, I. L. Aleiner, A. D. Mirlin, and D. G. Polyakov, Phys. Rev. B **71**, 115316 (2005).
[14] I. A. Dmitriev, A. D. Mirlin, and D. G. Polyakov, Phys. Rev. B **75**, 245320 (2007).
[15] S. Wiedmann, G. M. Gusev, O. E. Raichev, T. E. Lamas, A. K. Bakarov, and J. C. Portal, Phys. Rev. B **78**, 121301(R) (2008).
[16] J. Jo, Y. W. Suen, L. W. Engel, M. B. Santos, and M. Shayegan, Phys. Rev. B **46**, 9776 (1992).
[17] S. P. Shukla, Y. W. Suen, and M. Shayegan, Phys. Rev. Lett. **81**, 693 (1998).
[18] O. E. Raichev, Phys. Rev. B **78**, 125304 (2008).
[19] N. C. Mamani, G. M. Gusev, E. C. F. da Silva, O. E. Raichev, A. A. Quivy, and A. K. Bakarov, Phys. Rev. B **80**, 085304 (2009).
[20] G. F. Giuliani and J. J. Quinn, Phys. Rev. B **26**, 4421 (1982).
[21] Y. Berk, A. Kamenev, A. Palevski, L. N. Pfeiffer, and K. W. West, Phys. Rev. B **51**, 2604 (1995); M. Slutzky, O. Entin-Wohlman, Y. Berk, A. Palevski, and H. Shtrikman, *ibid.* **53**, 4065 (1996).
[22] A. T. Hatke, M. A. Zudov, L. N. Pfeiffer, and K. W. West, Phys. Rev. Lett. **102**, 066804 (2009).
[23] J.-Q. Zhang, S. Vitkalov, A. A. Bykov, A. K. Kalagin, and A. K. Bakarov, Phys. Rev. B **75**, 081305(R) (2007); J. Q. Zhang, S. Vitkalov, and A. A. Bykov, *ibid.* **80**, 045310 (2009).
[24] N. C. Mamani, G. M. Gusev, O. E. Raichev, T. E. Lamas, and A. K. Bakarov, Phys. Rev. B **80**, 075308 (2009).
[25] A. V. Goran, A. A. Bykov, A. I. Toropov, and S. A. Vitkalov, Phys. Rev. B **80**, 193305 (2009).
[26] K. W. Chiu, T. K. Lee, and J. J. Quinn, Surf. Sci. **58**, 182 (1976).
[27] S. A. Mikhailov, Phys. Rev. B **70**, 165311 (2004).
[28] C. B. Hanna and A. H. MacDonald, Phys. Rev. B **53**, 15981 (1996).